SCIENCE CHINA
Technological Sciences

November 2013 Vol.56 No.11: 2675–2680
doi: 10.1007/s11431-013-5376-1

Angular response of 'pin-hole' imaging structure measured by collimated β source

ZOU Hong[1*], LUO Lin[1], LI ChenFang[1], JIA XiangHong[2], XU Feng[2], CHEN HongFei[2], CHEN Jiang[1], SHI WeiHong[1], YU XiangQian[1] & ZOU JiQing[1]

[1] *Institute of Space Physics and Applied Technology, School of Earth and Space Science, Peking University, Beijing 100871, China;*
[2] *State Key Laboratory of Space Medicine Fundamentals and Application, Chinese Astronaut Research and Training Center, Beijing 100093, China*

Received April 23, 2013; accepted September 16, 2013; published online September 24, 2013

The pitch-angle distribution of energetic particles is important for space physics studies on magnetic storm and particle acceleration. A 'pin-hole' imaging structure is built with the 'pin-hole' technique and a position sensitive detector, which can be used to measure the pitch angle distribution of energetic particles. To calibrate the angular response of the 'pin-hole' imaging structure, special experiment facilities are needed, such as the particle accelerator with special design. The features of this kind of particle accelerator are: 1) The energy range of the outgoing particles should be mid-energy particles (tens keV to several hundred keV); 2) the particle flux should be consistent in time-scale; 3) the directions of the outgoing particles should be the same and 4) the particle number within the spot should be low enough. In this paper, a method to calibrate the angular response of the 'pin-hole' imaging structure by the $^{90}Sr/^{90}Y$ β source with a collimator is introduced and simulated by Geant4 software. The result of the calibration with the collimated β source is in accord with the Geant4 simulations, which verifies the validity of this method.

'pin-hole' imaging, Energetic particle, Pitch-angle distribution, Angular response, β source, Geant4 simulation

Citation: Zou H, Luo L, Li C F, et al. Angular response of 'pin-hole' imaging structure measured by collimated β source. Sci China Tech Sci, 2013, 56: 2675–2680, doi: 10.1007/s11431-013-5376-1

1 Introduction

Since the earth radiation belt was discovered by Van Allen in 60 s last century, particles with energy range from keV to MeV have been a focused area of research for several years. Energetic particles exist in various regions of the magnetosphere, which plays an important role in many space physics phenomena such as aurora, magnetic storm, the high energy electron bursts and so on [1, 2], and is a key factor in the energy coupling and transfer process of the solar wind-magnetosphere-ionosphere (SMI) system. The source and the acceleration mechanism of energetic particles are the two fundamental and unresolved scientific questions in the magnetospheric study [3]. The pitch-angle distribution of energetic particles is closely related with these questions and is a significant basis for the research of magnetospheric physics progress [4–9]. In addition, electron with high energy above MeV is one of the most serious threats to the spacecraft in the terrestrial space [10]. To understand the pitch angle distribution of energetic particles is the basis to accurately assess the space radiation environment and to establish a dynamic radiation belt model. Therefore, the measurement of the pitch-angle distribution of energetic particles is of great importance to scientific study and space

*Corresponding author (email: derakzou@aliyun.com)

© Science China Press and Springer-Verlag Berlin Heidelberg 2013

engineering.

In the past, 'top-hat' electrostatic analyzers [11] were generally used to measure the pitch-angle distribution of low energy particles, which can only measure the particles with energy less than 30 keV because of the high voltage restriction. An instrument with an array of solid-state position sensitive detector and a magnetic deflection system was carried by the CRRES spacecraft [12], which can measure 21–285 keV electrons and 7 keV–3.2 MeV protons from different directions. However, its angular range is confined by the magnetic field intensity and the size of the instrument. Moreover, magnetic flux leakage and weight are also the unfavorable factors in this design. In recent years, a new technology to achieve the measurement of pitch-angle distribution of energetic particles is the 'pin-hole' imaging structure technology. For example, the CEPPAD onboard POLAR [13] and RAPID onboard Cluster [14] both take this new structure for their merits of smaller in size and lighter in weight. An array position sensitive detector is arranged in the shielding box with a 'pin-hole' in the front end. Each detector cell and the 'pin-hole' consist of a particle telescope, which can measure the energy spectrum of energetic electrons incident from a certain direction. Therefore a 'pin-hole' box covers a wider incident angle. The combination of several similar structures can measure energetic particles in a 2π pitch angle. In the RAPID instrument, a three-cell position sensitive detector and a 'pin-hole' form a 'pin-hole' imaging structure, with each structure covering a 60° incident angle. The three structures can measure energetic electrons from 9 different directions in a 180° polar angle range (each direction having a field angle about 20°). With the spin of the cluster satellite, the RAPID can scan the pitch angle distribution of energetic particles in a 4π solid angle.

The accurate measurement to the pitch angle distribution relies on the good angular response of the 'pin-hole' imaging structure, so the angular response calibration for the structure is necessary. The angular response test for the proton imaging spectrometer (IPS) of CEPPAD onboard Polar was made with 30 keV mono-energetic proton source [13]. Three mono-energy electron sources with energies at 60, 90 and 114 keV were used in the angular response test for the imaging electron spectrometer (IES) of RAPID onboard Cluster [14]. The results of these tests demonstrated that this kind of 'pin-hole' imaging structure has a very good angular response. The traditional electron gun or electron accelcrator can generate electron beam with good directionality, weak energy dispersion and energy range from tens keV to MeV, which is widely used in space weather study, especially for the satellite charging and discharging effects [15, 16]. However, this kind of electron source has some difficulties for the angular response calibration for the 'pin-hole' structure [17]: Firstly, the intensity of electron beam is too strong, which could damage the detector or saturate the electronics system; secondly, the beam stability is generally not so good for the weak beam intensity; at last, the cost to run the equipment is too high for the long-term test. Some special methods can be used to overcome these disadvantages: The intensity of electron beam can be declined by scattering devices [18], but this will lead to a directional dispersion. The focusing and energy selecting technology can be used to improve the directionality and monochrome of the beam. However, this technology will make the system complex and increase the cost.

A method to measure the angular response of 'pin-hole' imaging structure by collimated β source is presented in this paper. And Geant4 software is adopted to simulate the angular response of the 'pin-hole' structure. The result of the calibration with the collimated β source is in accord with the Geant4 simulations, which verifies the validity of this method.

2 'Pin-hole' imaging structure

The schematic cross-section of a 'pin-hole' imaging structure is shown in Figure 1.

There are a 2 mm thickness copper plate and a 1 mm stainless steel which form the front shielding structure. The two layer metal plates with a platform gap are placed face to face to form a front-end pin slit structure. The equivalent shielding thickness of the side and back structure is about 3 mm (copper). A 1000 μm silicon solid-state detector array is arranged behind the pin slit in the box to form a 'pin-hole' imaging structure. The detector plane is parallel with the front-end shielding layer and its symmetric axis passes through the center of the 'pin-hole'. Three detector cells D1, D2, D3 form the particle telescope system with the pin-slit respectively, which divides the open angle θ into three field angles $\theta 1$, $\theta 2$ and $\theta 3$. According to the real size of the 'pin-hole' structure, the total open angle θ is about 56.2° and the field angle is about ~16.5° for each direction.

Each detector together with the rear-end electronics forms an individual signal channel. The system circuit diagram is shown in Figure 2. The system consists of a semi-

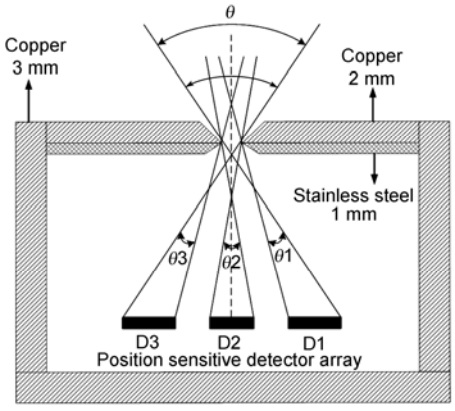

Figure 1 The schematic diagram of the 'pin-hole' imaging structure.

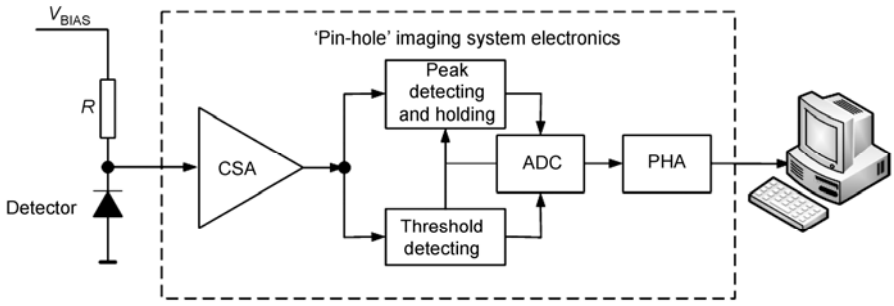

Figure 2 The block diagram of signal channel.

conductor detector, a charge sensitive amplifier (CSA), a peak detecting and holding circuit, a threshold detection circuit, an analog-to-digital conversion circuit and a pulse height analyzer (PHA). The particle signal generated by the detector is sent to the charge sensitive amplifier; the amplified signal is provided to the peak detecting and holding circuit and threshold detection circuit. If the amplitude of the particle signal exceeds the pre-defined threshold, the threshold detection circuit will trigger the peak detecting and holding circuit and ADC. The 12-bit digital signal of the ADC output is available to the PHA for the particle energy spectrum measurement. The data will be transferred to the test computer. The result will be analyzed and displayed on the computer in the end.

3 Geant4 simulation

Geant4 software [19] is a Monte-Carlo simulation toolkit which simulates the particle interactions with matter. It is widely used in high-energy physics, nuclear physics, high-power accelerators, etc. In space applications, Geant4 is introduced to simulate the effects of space radiation [20–22] and the particle detector design [23].

We use Geant4 to simulate the angular response of the 'pin-hole' structure. The incident electron source and the 'pin-hole' structure are shown in Figure 3. The range of incident angle is from −45° to +45°, taking the perpendicular line passing through the pin slit and D2 center as the reference 0° incident angle. At each incident angle, 100 keV electrons are uniformly sampled from the source plane with a 16 mm radius and the total electron number is 10^6. In Figure 3, the distance between the source plane and the 'pin-hole' is adjusted to show the system clearly.

In order to avoid the effect of scattering electrons, we choose electrons whose energy-loss in the three silicon detectors exceeds 40 keV as the effective particles in data statistics. The variations of the electron counts in the three detectors with incidence angle are shown in Figure 4.

From Figure 4, we can see that the angular response curves of the three detectors are similar: The counts keep at a high level within a certain incident angle; however, as the

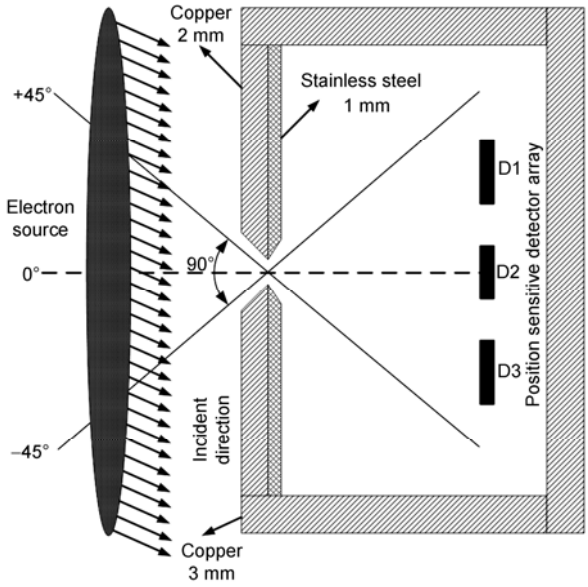

Figure 3 The equivalent cross-section of the 'pin-hole' structure in the horizontal direction and the incidence range of the simulated particles. The dash line, passing through the center of the pin slit and D2, represents the 0° incidence angle.

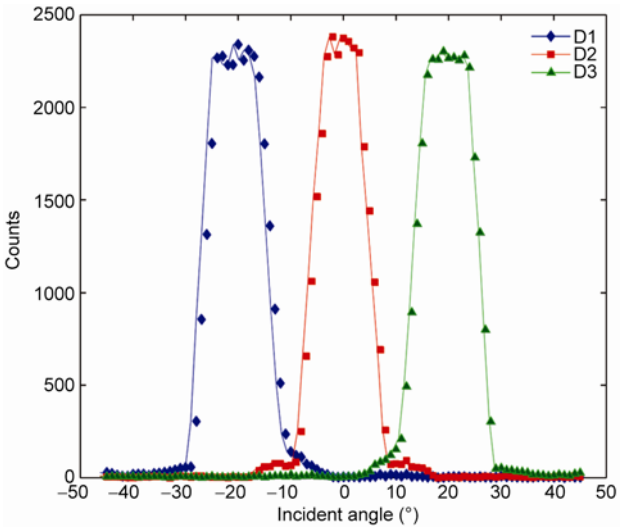

Figure 4 The electron counts of detectors D1/D2/D3 with different incidence angles.

incident angle is out of the range, the counts reduce to the background level which is caused by scattering. In the angular response curve of the middle detector (D2), the count values are slightly above the background level even the incidence angle is out of the field angle (~16.5°). The reason for this feature is that electrons hit on the 'pin-hole' edge and produce the electron scattering. The counts caused by scattering is an order of magnitude smaller than the high level counts within the field angle, so the scattering does not affect the angular response of the 'pin-hole' imaging system.

The peak incident angle of three response curves are ~−20°(D1), ~0°(D2) and ~+20°(D3), respectively. All the full widths at half maximum (FWHM) of the three response curves are less than 20°, which matches the theoretical value for the geometry of the 'pin-hole' imaging structure. Therefore, the Geant4 simulation demonstrates that our 'pin-hole' imaging structure has a good angular response for incident electrons.

4 Angular response verification by collimated β source

In order to verify the angular response of the 'pin-hole' imaging structure further, we tested it with collimated β source as shown in Figure 5.

The sensor is fixed on the rotatable platform, which can be accurately adjusted in 360° (the adjustment accuracy is 0.1°). The center of the pin slit coincides with the center of the rotatable platform and the plane of the pin slit is perpendicular to the rotating plane. Both of these conditions ensure the center of the pin slit is in a fixed position as the platform rotates.

We choose ^{90}Sr-^{90}Y as β source for its continuous energy spectrum, which is a good simulation to the electron spectrum of outer radiation belt [17]. In addition, the half-life of this radioactive source is long enough for a long time of radiation experiment with low operating cost, as often used in the internal charging and discharging test. In our test, the active area of ^{90}Sr-^{90}Y source (disc-plane source) is ~1 cm^2, which emits the mean flux of electron to about 3.12×10^6 in 2π solid angle. The material of the cylindrical collimator is lead (Pb). To confine the direction of the outgoing particle, a through-hole with a 1 mm diameter is drilled at the center of the front-end collimator whose wall thickness is 7 mm. The field angle of the quasi-unidirectional outgoing electron is about 16° for this collimator structure.

An Orteck multi-channel analyzer (MCA) and a 1000 μm Si-PIN detector are used to measure the energy spectrum of the collimated β source, as shown in Figure 6. It is demonstrated that the spectrum of the β source with collimator is between 50 and 500 keV, which matches well with the energy range of our 'pin-hole' detector (50–600 keV). The maximum count for each channel is less than 140 within 1 h (accumulating time), which shows that the collimator could weaken the source intensity, so it would not damage the detector or saturate the signal channel. Moreover, ^{90}Sr-^{90}Y generates a steady β stream and has a long half-life (about 28 years), so this source is very suitable for the angular response test.

The cylindrical collimator is fixed on a specimen holder. The symmetry axis of the collimator is parallel to the rotating platform and passes through the center of the pin slit, so as the platform rotates, the centers of the collimator open hole and the 'pin-hole' keep in the line of the symmetry axis, and the distance between the two centers keeps unchanged (15 mm). As shown in Figure 5, we define the incident angle to be 0° as the symmetry axis of the collimator is perpendicular to the 'pin-hole', the incident angle is positive as the platform rotates clockwise and is negative otherwise. Considering the field angle of the 'pin-hole' structure (~60°), the incident angle is set to change from −40° to +40°. The field angle of the collimator is about 16°. At 0° incident angle, the collimated β source covers an area with the center at the center of 'pin-hole' and the radius about 2.6 mm. Therefore, within the selected incident angle range, the outgoing electrons from the collimator can cover all the 'pin-hole' (1 mm×2 mm) area to avoid counting error caused by the limited field angle of the collimated β source.

To obtain the angular response of each detector cell (D1, D2 or D3), the total count of every detector is recorded within the same accumulation time (the accumulation time is chosen to be 10 min in the test, which relates to the source intensity and the open hole of the collimator) at a different incident angle. The incident angle varies in 2°. The variation of the total count of each detector accumulated in the same time with the incident angle is the angular response curve. For comparison, the normalized angular response curves obtained in the collimated β source test and the Geant4 simulation are shown in Figure 7. Although the results are generally consistent with each other, some differences also exist: The peak of the curve obtained in Geant4 simulation is flatter, which means that the counts

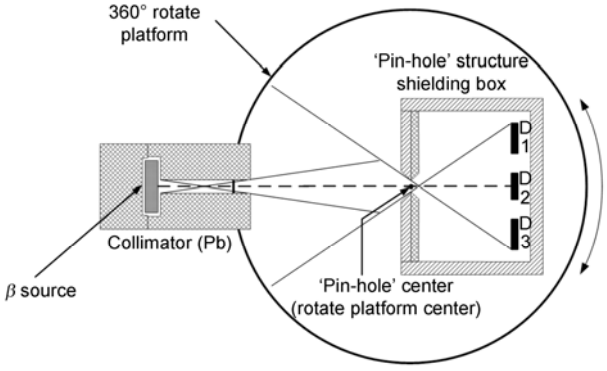

Figure 5 The diagram of the angular response test of the 'pin-hole' imaging structure by collimated β source. Three silicon detectors are presented as D1, D2 and D3 respectively.

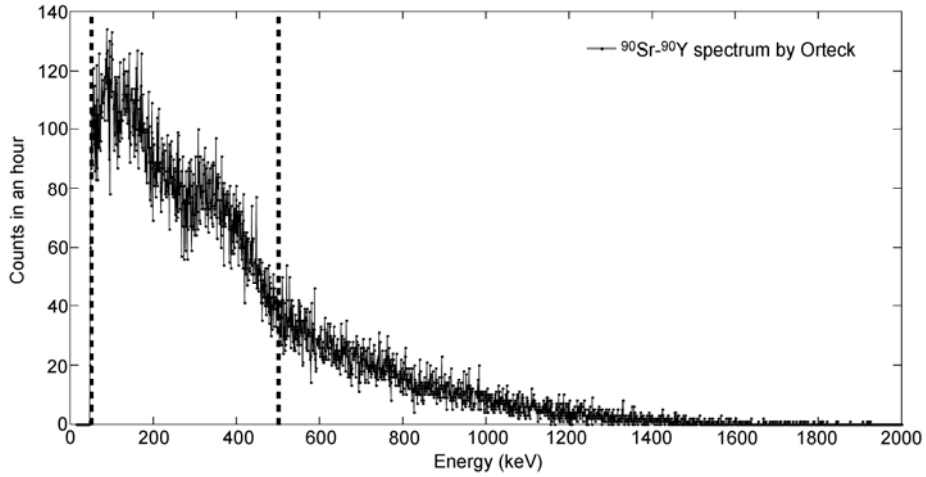

Figure 6 The energy spectrum (dotted line) from a collimated ^{90}Sr/^{90}Y radioactive source obtained with 1000 μm Si-PIN detector and Orteck multichannel analyzer. The abscissa is energy in keV, the ordinate is the count accumulated within 1 h. The region between the two dash lines is the energy range from 50 to 500 keV.

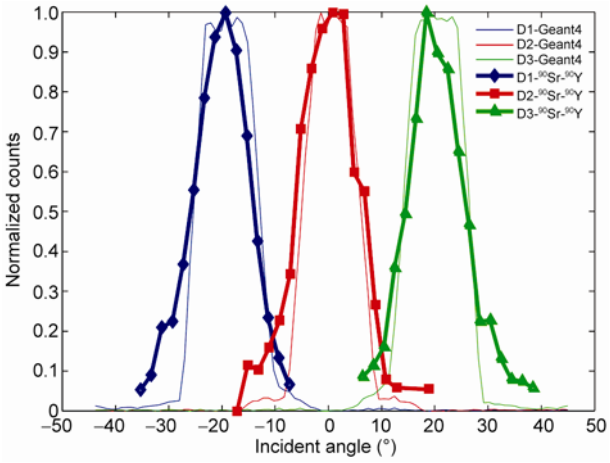

Figure 7 The normalized angular response curves of the three detectors D1 (blue line), D2 (red line) and D3 (green line) obtained in the collimated β source test and the Geant4 simulation test. The fine line is the results of Geant4 analysis and the heavy line is the results of β source test.

keep at a high level in a certain range of incident angle and decrease rapidly outside of the range. Whereas the peak of the curve obtained in the collimated β source test is sharper and the counts outside the peak (the normalized count is less than 0.4) are higher than the Geant4 results. The main cause of this difference should be the different electron sources used in the two tests. In the Geant4 simulation test, the directions of the incidence electrons are the same. However, the electrons emitted from the active region of the radioactive source are generally isotropic in the 2π solid angle. With the collimator, the outgoing electrons are conically distributed and the directions cannot be the same.

To further validate the results of the collimated β source test, we changed the electron plane source to cone source in Geant4 simulation. Figure 8 shows the incidence of the electrons from the two sources into the 'pin-hole' imaging structure.

We re-counted the angular response of the 'pin-hole' imaging structure by using cone electron source and the results are shown in Figure 9. Comparing Figure 7 and Figure 9, the simulation results with cone electron source matc-

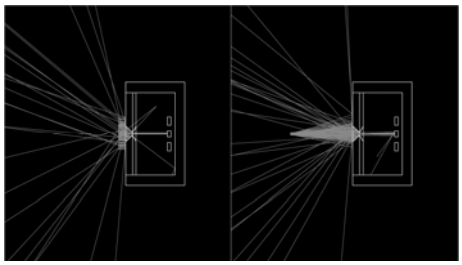

Figure 8 Diagram of the incidence of the electrons from two sources into the 'pin-hole' imaging structure. The left is plane electron source with consistent direction (we reduce the area of the source and increase the distance between the source and the front surface of the 'pin-hole' structure to 2 mm in order to display well), the incident angle is 0°; the right is cone source with the 0° center incident angle.

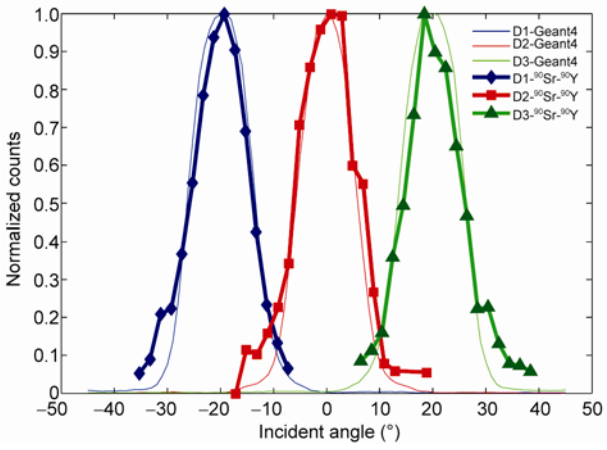

Figure 9 The normalized angular response curves of the three detectors D1 (blue line), D2 (red line) and D3 (green line) are obtained in the collimated β source test and the Geant4 simulation test with cone electron source. The fine line is the results of Geant4 analysis and the heavy line is the results of β source test.

Table 1 The incident angles and field angles of the three detectors obtained by three methods

Detector cell	Incident angle range (°)			Field angle (°)		
	Theoretical calculation	GENAT4 simulation	Calibration test	Theoretical calculation	GENAT4 simulation	Calibration test
D1	−28.6 − −11.8	−26.9 − −12.7	−26.7 − −12.8	16.8	14.2	13.9
D2	−8.1 − 8.1	−6.6 − 6.7	−6.6 − 7.8	16.2	13.3	14.4
D3	11.8 − 28.6	12.6 − 26.9	12.9 − 26.9	16.8	14.3	14.0

hes the results of the collimated β source much better, which verifies that the result of the collimated β source is credible.

A summary about the incident range and filed angle is shown in Table 1 in three aspects: The theoretical calculation according to the structure geometry, the Geant4 simulation and the calibration test with collimated $^{90}Sr/^{90}Y$ radioactive source. All the results match well with each other and the angular resolution is less than 20°. The test results have shown that our 'pin-hole' structure can distinguish the electrons incident from different directions.

5 Conclusions

In this paper, a 'pin-hole' imaging structure is designed for the imaging energetic electron spectrometer. A method to measure the angular response of the 'pin-hole' structure with collimated 90Sr/90Y β source is introduced. The angular response of this structure is simulated with Geant4 software. The collimated β source is used in the angular response test. Both of the results match well and demonstrate the validity of this method. It also certifies that our 'pin-hole' imaging structure has a good angular resolution.

This work was supported by the National Natural Science Foundation of China (Grant Nos. 40704026 and 41374167).

1 Baker D N, Pulkkinen T I, Li X, et al. Coronal mass ejections, magnetic clouds, and relativistic magnetospheric electron events: ISTP. J Geophys Res, 1998, 103: 17279–17291
2 Reeves G D. Relativistic electrons and magnetic storms: 1992–1995. Geophys Res Lett, 1998, 25: 1817–1820
3 Baker D N, Elkington S R, Li X, et al. Particle Acceleration in The Inner Magnetosphere: Physics and Modelling. Washington D C: AGU, 2005. 73–85
4 Roberts C S. Pitch-angle diffusion of electrons in the magnetosphere. Rev Geophys, 1969, 7: 305–337
5 West Jr H, Buck R, Walton J. Electron pitch angle distributions throughout the magnetosphere as observed on Ogo 5. J Geophys Res, 1973, 78: 1064–1081
6 Morioka A, Misawa H, Miyoshi Y. Pitch angle distribution of relativistic electrons in the inner radiation belt and its relation to equatorial plasma wave turbulence phenomena. Geophys Res Lett, 2001, 28: 931–934
7 Horne R B, Meredith N P, Thorne R M, et al. Evolution of energetic electron pitch angle distributions during storm time electron acceleration to megaelectronvolt energies. J Geophys Res, 2003, 108: 1016
8 Summers D, Thorne R M. Relativistic electron pitch-angle scattering by electromagnetic ion cyclotron waves during geomagnetic storms. J Geophys Res, 2003, 108: 1143
9 Gannon J L, Li X, Heynderickx D. Pitch angle distribution analysis of radiation belt electrons based on CRRES MEA data. J Geophys Res, 2007, 112: 5212
10 Baker D N. How to cope with space weather. Science, 2002, 297: 1486–1487
11 Lin R P. A three-dimensional plasma and energetic particle investigation for the wind spacecraft. Space Sci Rev, 1995, 71: 125
12 Korth A, Kremser G, Wilken B, et al. Electron and proton wide-angle spectrometer (EPAS) on the CRRES spacecraft. J Spacecraft Rockets, 1992, 29: 609–614
13 Black J B. CEPPAD experiment on POLAR. Space Sci Rev, 1995, 71: 531
14 Wilken B. RAPID: The imaging energetic particle spectrometer on cluster. Space Sci Rev, 1997, 79: 399–473
15 Coakley P, Kitterer B, Treadaway M. Charging and discharging characteristics of dielectric materials exposed to low-and mid-energy electrons. IEEE Trans Nucl Sci, 1982, NS-29: 1639–1643
16 Han J W, Zhang Z L, Huang J G, et al. An environmental simulation facility for study of deep dielectric charging on satellites. Spacecraft Environ Eng, 2007, 24: 47–50
17 Ryden K A, Morris P A, Rodgers D J, et al. Improved demonstration of internal charging hazard using 'realistic electron environment facility (REEF). In: the Proc 8th Spacecraft Charging Technol Conf, Huntsville, 2003
18 Coakley P G, Treadaway M J, Robinson P A. Low flux laboratory test of the internal discharge monitor (IDM). IEEE Tran Nuc Sci, 1985, 32: 4066–4072
19 Agostinelli S, Allison J, Amako K, et al. Geant4-a simulation toolkit. Nuclear Instrum Meth Phys Res-Sec A, 2003, 506: 250–303
20 Gao B R, Hao Y Q, Jiao W X. A study on spacecraft internal charging with MONTE CARLO method. Chin J Space Sci, 2004, 24: 289–294
21 Allison J, Amako K. Geant 4 developments and applications. IEEE Trans Nuc1 Sci, 2006, 53: 270–278
22 Hao Y Q, Jiao W X, Chen H F. A Monte carlo study on internal charging of onboard subsystem during the July 2004 energetic electron event (in Chinese). Prog Geophys, 2009, 24: 1937–1942
23 Li X C, Chen H F, Hao Y Q, et al. Investigation of electrons inside the satellite by the Geant4 simulation. Sci China Tech Sci, 2011, 54: 2271–2275